NUCLEAR THEORY, Vol. 29 (2010)
eds. A. Georgieva, N. Minkov, Heron Press, Sofia

Microscopic Description of Ground and One-Quasiparticle States in Neutron-Rich Sr, Zr and Mo Isotopes with the Gogny Energy Density Functional

R. Rodríguez-Guzmán[1], **P. Sarriguren**[1], **L.M. Robledo**[2]

[1]Instituto de Estructura de la Materia, CSIC, Serrano 123, E-28006 Madrid, Spain
[2]Departamento de Física Teórica, Universidad Autónoma de Madrid, 28049-Madrid, Spain

Abstract. The evolution of the ground state nuclear shapes in neutron-rich Sr, Zr and Mo isotopes, including both even-even and odd-A nuclei is discussed within the mean field approximation based on the Gogny-D1S Energy Density Functional. Charge radii as well as neutron separation energies are calculated and compared with available data. A correlation between a shape transition and a discontinuity in those observables is found. Odd nuclei are considered within the so called Equal Filling Approximation which is also used to test the spectroscopic quality of the Gogny-D1S functional to reproducing the trends observed in the systematics of low-lying one-quasineutron configurations for odd-N isotopes of the considered region of the nuclear chart.

1 Introduction

In this work, we illustrate one of our recent applications [1] of the Hartree-Fock-Bogoliubov (HFB) approximation, based on the Gogny-EDF (parametrization D1S [2]). In particular, we pay attention to the evolution of nuclear shapes, and the structural changes associated with it, in neutron-rich Sr, Zr and Mo isotopes. To this end, we will concentrate on selected (even-even and also odd-A) nuclei with neutron numbers $46 \leq N \leq 68$. One should keep in mind that, even when they roughly constitute half of the existing nuclides, odd nuclei have been much less studied that their even counterparts. Nevertheless, the properties of odd nuclei are very relevant to understand odd-even effects related to pairing correlations as well as to constraint EDFs aiming to reach a reasonable spectroscopic quality. Due to this there is a growing interest in the properties of odd nuclei (see, for example, [3, 4]).

The election of the considered Sr, Zr and Mo nuclei is mainly driven by the intense experimental [5–11] and theoretical [1, 12, 13] efforts to better understand this region of the nuclear chart playing an essential role to model the

r-process in a reliable way [14] and also characterized by the strong competition between various shapes [1, 15]. In addition, masses and charge radii data available for Sr, Zr and Mo nuclei [5, 8, 11, 16] are considered among the most sensitive observables to explore the structural evolution far from the valley of stability, where other types of spectroscopic experiments are prohibitive because of the low production rates and short lifetimes of unstable isotopes. In particular, discontinuities in the systematics of masses suggest a change in the structure of the ground states and drastic changes in the mean square (ms) radius of the charge distributions in regions of transitional nuclei may also be indicators of structural changes related to the nuclear deformation [1, 5, 8, 11, 16].

2 Theoretical Framework

In order to study the evolution of the ground state shapes as well as the systematics of the one-quasineutron configurations in odd-A Sr, Zr and Mo nuclei we have used the HFB approximation [17]. Ground state deformations are obtained self-consistently but we have also constructed (even-even isotopes) potential energy curves (PEC) or potential energy surfaces (PES) to obtain first hints on the evolution with the number of nucleons of the various competing shapes [1]. This has been accomplished preserving axial symmetry and also allowing afterward for triaxiality (in the most relevant isotopes). Hence, we have constrained the mean value of the quadrupole operators $\hat{Q}_{20}$ and $\hat{Q}_{22}$ (in the axial case only the former is constrained) along the lines discussed in references [17, 18]. For the description of odd-A nuclei, we have considered blocked (one-quasiparticle) HFB wave functions $|\Phi_{\rm HFB}\rangle_\alpha = \beta^+_\alpha |\Phi_{\rm HFB}\rangle$ with α standing for the quantum numbers characterizing the blocked state (angular momentum projection K and parity in the case of axial symmetry). To preserve time-reversal, the ground and one-quasiparticle configurations of an odd nucleus are obtained within the HFB Equal Filling Approximation (EFA) [1, 3] which has already been shown to be sufficiently precise for most practical applications [4].

3 Evolution of Nuclear Shapes in Neutron-Rich Sr, Zr and Mo Isotopes

From the computation of the PECs, the main features of the shape evolution in the axial case can be summarized as follows: The isotopes with $N = 50 - 54$ show a sharp PEC around the spherical minimum that becomes rather shallow at $N = 56 - 58$. Isotopes with $N = 60$ are already deformed with oblate and prolate minima very close in energy. In the case of Sr isotopes the ground state is prolate, for Zr isotopes both oblate and prolate minima are found at about the same energy, while for Mo isotopes the ground state is oblate. Beyond $N = 60$ the shapes become stable and for heavier isotopes we obtain basically similar results to $N = 60$. It is also worth mentioning the incipient emergence of a spherical solution in the heavier isotopes. Our results agree well with the

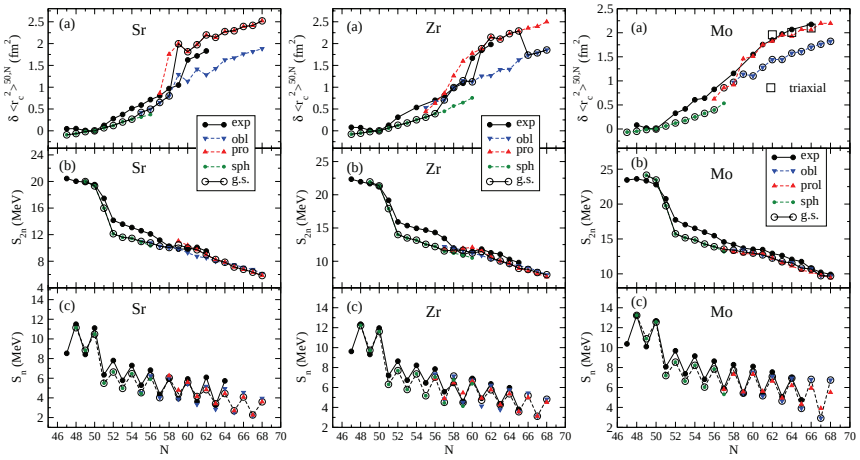

Figure 1. Calculated $\delta\langle r_c^2\rangle$ (a), S_{2n} (b), and S_n (c) in Sr, Zr and Mo isotopes compared to experimental data. Results for prolate, oblate, and spherical minima are displayed with different symbols (see legend). Open circles correspond to ground-state results. For more details, see main text.

shape/phase changes predicted around $N = 60$ in previous works [12, 13, 19–21].

In Figure 1 we can see the results obtained [1] for the charge radii differences $\delta\langle r_c^2\rangle^{50,N} = \langle r_c^2\rangle^N - \langle r_c^2\rangle^{50}$ in (a), for the two-neutron separation energies S_{2n} in (b), and for the one-neutron separation energies S_n in (c) as a function of the neutron number N for the considered Sr, Zr and Mo nuclei. Experimental data have been taken from [5, 8, 11, 16]. Besides the abrupt decrease of S_{2n} and S_n at $N = 50$ corresponding to the shell closure, the evolution of the S_{2n} and S_n along the isotopic chains shows a change in the tendency around $N = 60$ in Sr and Zr isotopes. This suggests a change in the ground-state shape of these isotopes. On the other hand, the chain of Mo isotopes shows a smoother behavior. These observations are confirmed by laser spectroscopy experiments in which the shape change in Sr and Zr is observed in the form of a sudden increase of the ms charge radii at $N = 58 - 60$ while the Mo isotopic chain displays a smooth behavior [11] as N increases.

In Figure 1 we also see the calculated values using the oblate (down triangles), prolate (up triangles) and spherical (dots) shapes corresponding to the local minima in the PECs. We also plot by open circles the theoretical values that correspond to the ground states of the corresponding isotopes. In general, the measured S_{2n} are reproduced reasonably well. The calculated shell gap at $N = 50$ is larger than observed, but this is a well known feature related to any mean-field calculation. The discrepancy can be reduced considering dynamical correlations beyond mean field [20, 21]. Between $N = 52$ and $N = 58$, the S_{2n} energies are underestimated by the calculations, while they are much better

reproduced beyond $N = 60$.

In our calculations a change in the tendency is observed at $N \sim 60$, which is more pronounced in Sr and Zr isotopes and almost disappears in Mo isotopes. However, the shoulder is less apparent than the experimental one due to the underestimation of the data below $N = 60$. In the case of S_n energies, the amplitude of the odd-even staggering in S_n is well reproduced by the calculations indicating the validity of our theoretical description of odd-A nuclei. In general, the agreement is fairly good below $N = 50$. Then, the calculations underestimate the measured S_n values between $N = 50$ and $N = 60$, being the net effect a displacement to slightly lower energies. The agreement improves substantially for heavier isotopes.

The evolution of the nuclear charge radii differences $\delta\langle r_c^2\rangle^{50,N}$ can be seen in panels (a) of Figure 1. For Sr isotopes, the calculations follow nicely the measurements with a smooth increase of $\delta\langle r_c^2\rangle$ up to $N = 58$, then a sudden jump occurs at $N = 60$ and again the increase is smooth for heavier isotopes. The encircled symbols indicate the shapes corresponding to the ground states obtained in our calculations. We can see that the lighter isotopes are spherical, then they change into oblate very smoothly and at about $N = 60$ they become prolate. The observed jump corresponds to the transition from the oblate to the prolate shape. For Zr isotopes, the spherical shapes account for the behavior of $\delta\langle r_c^2\rangle^{50,N}$ up to $N = 56$. From $N = 56$ up to $N = 60$ there is a smooth transition to oblate shapes that become the ground states and reproduce quite well the experiment. Above $N = 60$ we obtain prolate ground states with radii in agreement with the observed jump. For heavier isotopes (beyond $N = 66$) we obtain again oblate shapes but there is no information in this region. Finally, the lightest Mo isotopes are spherical changing into oblate shapes and increasing $\delta\langle r_c^2\rangle^{50,N}$ very smoothly.

The neutron and proton single-particle energies (SPE) shown in Figures 2 and 3 for the nucleus ^{102}Zr as functions of the axial quadrupole moment Q_{20} help us to identify the regions of low level density, which favor the onset of deformation (Jahn-Teller effect [23]), as well as to stress the important role of the interplay between the proton $\pi g_{9/2}$ and the neutron $\nu h_{11/2}$ orbitals (Federman-Pittel effect [24]) to generate deformed configurations [17, 18]. For the proton SPEs we observe an energy gap below the Fermi level at $Q_{20} \approx 5$ b, which favors the onset of prolate deformation in Sr isotopes. On the other hand, above the Fermi energy, the low level density on the oblate sector favors oblate configurations in Mo isotopes. In the case of neutron SPEs the energy gap below the Fermi level at $Q_{20} \approx -2.5$ b favors oblate shapes in lighter isotopes ($N < 60$), whereas the energy gap above the Fermi level at $Q_{20} = 5$ b favors prolate shapes in heavier isotopes ($N > 60$). Thus, these simple ideas offer a qualitative understanding of the various mechanisms leading to deformation in this mass region [1] .

In general, we observe that the predicted spherical ground states from $N = 54 - 60$ underestimate the data for $\delta\langle r_c^2\rangle^{50,N}$ in the three isotopic chains but

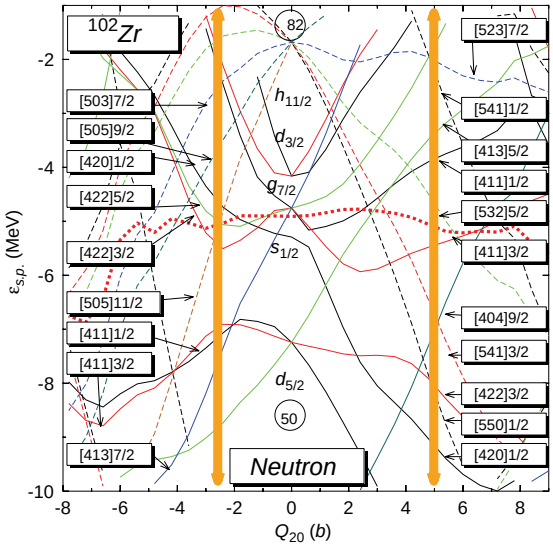

Figure 2. Single particle energies for neutrons in ^{102}Zr as a function of the axial quadrupole moment Q_{20}. The Fermi level is depicted as a thick dashed red line. The results have been obtained with the Gogny-D1S EDF. Solid lines correspond to levels with positive parity whereas dashed lines correspond to negative parity states. Asymptotic (Nilsson) quantum numbers $[N, n_z, \Lambda]K^\pi$ are shown for Q_{20} values close to those where the minima of the PECs are located (vertical arrows).

a possible explanation for the discrepancy could be that configuration mixing plays an important role in these isotopes [21, 22]. In the case of Sr isotopes, the sudden change in $\delta\langle r_c^2\rangle^{50,N}$ occurs experimentally between $N = 59$ and $N = 60$, whereas theoretically it appears between $N = 58$ and $N = 59$. Similarly in Zr isotopes we obtain the change between $N = 60 - 61$, while experimentally is observed between $N = 59 - 60$. We do not think this discrepancy is significant since it is related to the subtle competition between prolate and oblate shapes. We should notice that in the isotopes where the shape is changing we get practically degenerate energies for oblate and prolate deformations and thus, tiny changes in the details of the calculations can lead to a different ground state. In the case of the heavier Mo isotopes we also recognize a difficulty in the reproduction of the data since the oblate shapes, which are the ground states, underestimate them. However, we can see that the prolate shapes, which are close in energy, agree with the data. To get a further insight, we have performed triaxial calculations [17, 18] for the critical isotopes around $N = 60$ [1]. As a result of these calculations, we observe how in Sr and Zr isotopes the transition from oblate to prolate at $N = 60$ is manifest, suddenly changing from deformations of ~ 2 b in the oblate sector to ~ 5 b in the prolate one. On the contrary, for Mo isotopes the oblate shape at $N = 58$ becomes gradually triaxial as N increases

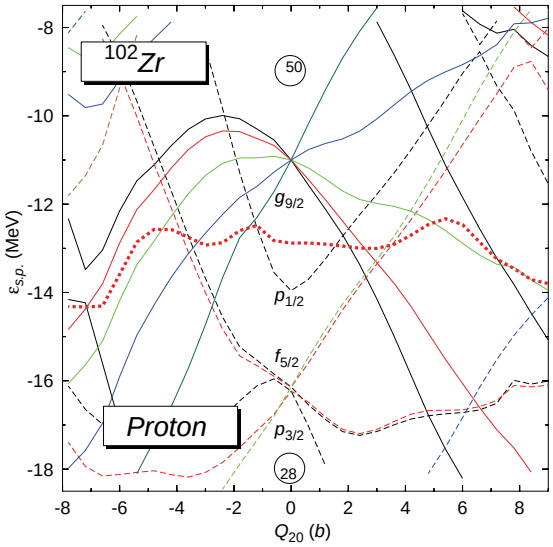

Figure 3. The same as Figure 2 but for protons.

(i.e., an island of triaxiality is apparent from $N = 60$ up to $N = 68$). We have calculated the charge radii corresponding to these triaxial configurations that become ground states and have added them in Figure 1 with open squares. The new $\delta\langle r_c^2\rangle^{50,N}$ values for these Mo isotopes are now very close to the axial-prolate values and agree very nicely with the experiment. One should notice that one important ingredient for the agreement achieved [1] is that the location of the triaxial minima is much closer to the axial prolate minima than to the oblate ones, which are lower.

Now, we turn our attention to the systematics of one-quasiparticle configurations in the considered odd-A Sr, Zr and Mo isotopes. To this end, as an illustrative example, in Figure 4 the experimental (a) excitation energies and spin-parity assignments of the one-quasineutron states in odd-N Zr isotopes are compared with our HFB-EFA predictions (b). The lighter Zr isotopes ($A = 87 - 95$), show spherical equilibrium shapes, which turn into oblate ($A = 97, 99$), prolate ($A = 101 - 105$), and again oblate ($A = 107$) ground states with excited one-quasiparticle configurations of different shapes below 1 MeV and very close in energy.

The structural evolution of the ground and excited one-quasiparticle states along the Zr isotopic chain can be followed by looking at the dashed lines connecting the states characterized by the same asymptotic quantum numbers $[N, n_z, \Lambda]K^\pi$ and at Figure 2, as a guide. In fact, the dashed lines in Figure 4 are also useful to trace the isotopic evolution of the single-particle configurations, which can be also understood by moving the (neutron) Fermi level in Figure 2 through the vertical arrows.

Thus, taking for example the prolate solutions, if one looks at the orbitals intersecting the vertical arrow at $Q_{20} = 5$ b in Figure 2, one finds the deepest state at about $e_{sp} = -9$ MeV, which corresponds to a $[420]1/2^+$ $(s_{1/2})$ state. It can be seen, in Figure 4, as the prolate excited state at 0.6 MeV in ^{95}Zr. The next prolate states in Figure 2 are $[550]1/2^-$ falling down very quickly from $h_{11/2}$ and $[422]3/2^+$ $(d_{5/2})$ appearing as the first prolate excitations in ^{97}Zr. On the other hand, in ^{99}Zr the first two prolate states $3/2^-$ and $9/2^+$ appear

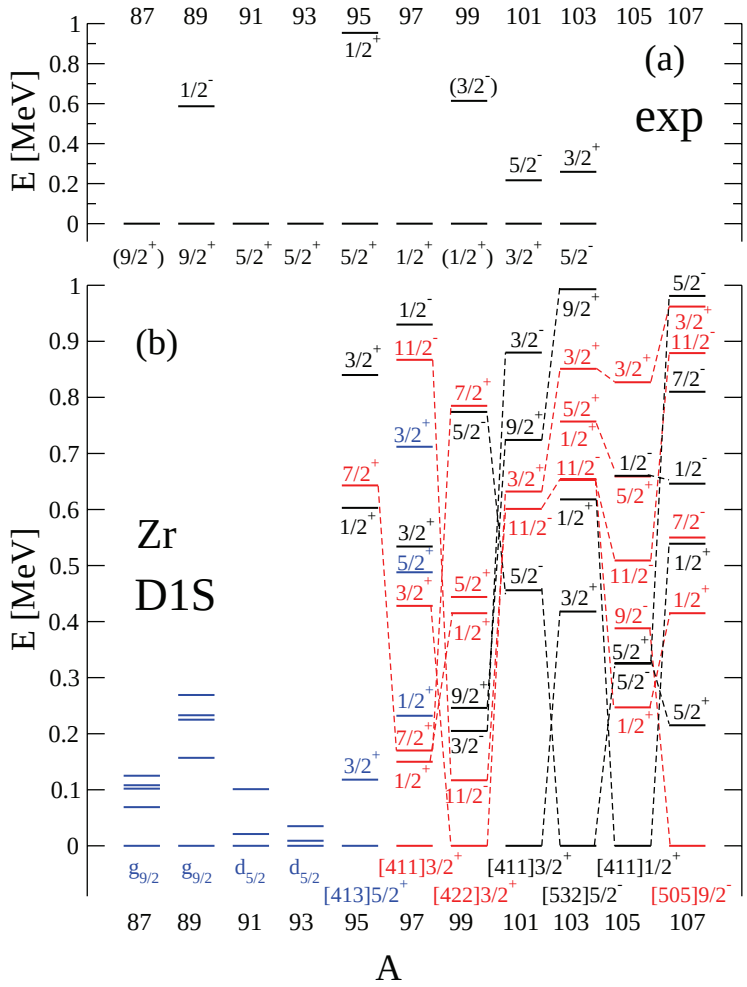

Figure 4. Experimental (a) excitation energies and spin-parity assignments of the non-collective states are compared with HFB-EFA results (b) for the one-quasineutron states in odd-N Zr isotopes (see text for details). Prolate configurations are shown by black lines, oblate ones by red lines, and spherical ones by blue lines.

around 0.2 MeV. They are associated with the $[541]3/2^-$ coming down from $h_{11/2}$ and $[404]9/2^+$ raising from $g_{9/2}$ in Figure 2. Going further up in Figure 2 we find $[411]3/2^+$ $(g_{7/2})$, which is the ground state in ^{101}Zr and $[532]5/2^-$ $(h_{11/2})$ which represents an excited state at about 0.45 MeV. Further up in excitation energy one finds, the $9/2^+$ and $3/2^-$ states already discussed (see the connections with dashed lines with their partners in ^{99}Zr). In ^{103}Zr the $3/2^+$ and $5/2^-$ states interchange their positions with respect to ^{101}Zr and, as it can be easily understood from Figure 2, the $[532]5/2^-$ configuration becomes now the ground state. Subsequently, the $[411]1/2^+$ $(g_{7/2})$ ground state is predicted by our HFB-EFA. The excited one-quasineutron $5/2^-$ and $5/2^+$ states, at about 0.35 MeV, correspond to the already discussed $[532]5/2^-$ $(h_{11/2})$, which now lies below the Fermi level, and to the $[413]5/2^+$ $(d_{5/2})$ configuration, above the Fermi level, that becomes the lowest prolate deformed one-quasiparticle excitation in the last odd-N Zr isotope considered (i.e., ^{107}Zr).

A similar analysis can be made for the oblate one-quasineutron states by looking at the intersections of the single-particle levels in Figure 2 with the vertical line at $Q_{20} = -2.5$ b. As can be seen from Figure 4, ^{97}Zr displays a ground $3/2^+$ and two low-lying excited ($1/2^+$ and $7/2^+$) oblate deformed states. They can be associated with the three orbitals at -8 MeV in the oblate sector of Figure 2, namely, $[411]3/2^+$ $(d_{5/2})$, $[411]1/2^+$ $(d_{5/2})$, and $[413]7/2^+$ $(g_{7/2})$. Next, in ^{99}Zr we find an oblate $3/2^+$ ground state and the oblate $11/2^-$ excitation at 0.1 MeV which correspond to the $[422]3/2^+$ $(g_{7/2})$ and $[505]11/2^-$ intruder state coming down from the $h_{11/2}$ shell. The $[420]1/2^+$ and $[422]5/2^+$ (coming from $g_{7/2}$ shell) excitations , are also visible in the quasiparticle spectrum of ^{99}Zr. The nucleus ^{101}Zr exhibits a prolate ground state but one finds a $[505]11/2^-$ as the lowest oblate quasineutron configuration very close to the $3/2^+$ excitation (that was the ground state in ^{99}Zr). The same comments apply to both ^{103}Zr and ^{105}Zr but now the state $[420]1/2^+$ $(s_{1/2})$ comes into play. Finally, ^{107}Zr displays an oblate ground state that can be associated with a $[505]9/2^-$ configuration coming down from the $h_{11/2}$ shell.

In general, we observe a reasonable agreement between the spin-parity systematics of one-quasineutron states predicted by our (parameter free) HFB-EFA, based on the universal EDF Gogny-D1S [2], and the available experimental data. The main difficulties to describe the experimental information appear in those cases where the mean field approach might not be sufficient. Such is the case of $N = 55 - 59$ isotopes, where we get very shallow minima, a situation that in general requires configuration mixing [22] for a better description. Difficulties also appear when the description requires the inclusion triaxility as for the heavier Mo isotopes, which exhibit a γ-soft behavior and even triaxial minima [1] with the axial ones converted into saddle points. In such a situation one also expects that the oblate and prolate solutions will be highly mixed. On the other hand, a HFB axial description is expected to work better for well developed axial minima separated by energy barriers in both spherical and triaxial shapes as in the heavier isotopes of Sr and Zr [1] .

4 Conclusion

Our primary aim in this contribution has been, to search for signatures of structural changes and shape transitions in Sr, Zr and Mo nuclei. We have found a remarkable connection between shape transitions and sudden changes in the behavior of the isotopic dependence of the nuclear charge radii. As compared to Sr and Zr isotopes, we have found that Mo isotopes exhibit a smoother increase in the charge radii with the number of neutrons, which is in good agreement with the experimental data. Triaxial degrees of freedom are required to get this agreement beyond $N = 60$.

Subsequently, we have also illustrated our results concerning the systematics of one-quasineutron configurations in the case of odd-N Zr isotopes. We are aware of the challange of reproducing the observed spectroscopic properties in the particular mass region considered but nevertheless we have obtained a positive answer to the question whether the Gogny-D1S EDF is able to reproduce the observed trends qualitatively and therefore to make predictions in unexplored regions. A beyond mean-field treatment seems to be necessary to improve the quality of the description in some cases, and configuration mixing calculations in the spirit of the Generator-Coordinate-Method (GCM) method [22] may be required to improve the mean-field results. We are still far from being able to apply such a configuration mixing approach within an exact blocking scheme for odd nuclei. Nevertheless, a HFB-EFA-GCM scheme can be considered as a plausible step forward in this direction and work along this lines is in progress.

Acknowledgements

This work was supported by MICINN (Spain) under research grants FIS2008–01301, FPA2009-08958, and FIS2009-07277, as well as by Consolider-Ingenio 2010 Programs CPAN CSD2007-00042 and MULTIDARK CSD2009-00064. We also thank Profs. J. Dobaczewski and J. Äysto and the experimental teams of the University of Jyväskylä (Finland) for encouraging discussions.

References

[1] R. Rodríguez-Guzmán, P. Sarriguren, L.M. Robledo and S. Perez-Martin, *Phys. Lett*. **B691** (2010) 202.
[2] J.F. Berger, M. Girod, and D. Gogny, *Nucl. Phys.* **A428** (1984) 23c.
[3] S. Perez-Martin, and L.M. Robledo, *Phys. Rev. C* **78** (2008) 014304.
[4] N. Schunck, *et al.*, *Phys. Rev. C* **81** (2010) 024316.
[5] F. Buchinger, *et al.*, *Phys. Rev. C* **41** (1990) 2883.
[6] H. Mach, *et al.*, *Nucl. Phys*. **A523** (1991) 197.
[7] W. Urban, *et al.*, *Nucl. Phys*. **A689** (2001) 605.
[8] P. Campbell, *et al.*, *Phys. Rev. Lett*. **89** (2002) 082501.
[9] H. Hua, *et al.*, *Phys. Rev. C* **69** (2004) 014317.
[10] C. Goodin, *et al.*, *Nucl. Phys*. **A787** (2007) 231c.

[11] F.C. Charlwood, *et al.*, *Phys. Lett*. **B674** (2009) 23.
[12] J. Skalski, S. Mizutori, and W. Nazarewicz, *Nucl. Phys*. **A617** (1997) 281.
[13] F. R. Xu, P. M. Walker, and R. Wyss, *Phys. Rev. C* **65** (2002) 021303(R).
[14] J. J. Cowan, F. -K. Thielemann, and J. W. Truran, *Phys. Rep*. **208** (1991) 267.
[15] J. L. Wood, K. Heyde, W. Nazarewicz, M. Huyse, and P. Van Duppen, *Phys. Rep*. **215** (1992) 101.
[16] U. Hager *et al.*, *Phys. Rev. Lett*. **96** (2006) 042504.
[17] L.M. Robledo, R. Rodríguez-Guzmán and P. Sarriguren, *J. Phys. G: Nucl. Part. Phys*. **36** (2009) 115104.
[18] R. Rodríguez-Guzmán, P. Sarriguren, L.M. Robledo and J.E. García-Ramos, *Phys. Rev. C* **81** (2010) 024310.
[19] P. Möller *et al.*, *At. Data Nucl. Data Tables* **94** (2008) 758.
[20] M. Bender, G. F. Bertsch, and P.-H. Heenen, *Phys. Rev. C* **73** (2006) 034322; *ibid.* **78** (2008) 054312.
[21] J.-P. Delaroche, *et al.*, *Phys. Rev. C* **81** (2010) 014303.
[22] R. R. Rodríguez-Guzmán, J. L. Egido, and L.M. Robledo, *Nucl. Phys*. **A709** (2002) 201.
[23] P.-G. Reinhard and E.W. Otten, *Nucl. Phys*. **A420** (1984) 173.
[24] P. Federman and S. Pittel, *Phys. Lett*. **B69** (1977) 385; *Phys. Rev. C* **20** (1979) 820.